#### **Research Article**

Yue Li\* and Shaohua Zeng

# High strength, anti-static, thermal conductive glass fiber/epoxy composites for medical devices: A strategy of modifying fibers with functionalized carbon nanotubes

https://doi.org/10.1515/epoly-2023-0123 received August 12, 2023; accepted September 09, 2023

**Abstract:** A series of aliphatic amine-functionalized multiwalled carbon nanotubes (MWCNTs) wherein varied secondary amine numbers were grafted on the MWCNTs' surface were synthesized and further dispersed onto the glass fibers for reinforcing epoxy-based composites. By tuning secondary amine numbers of aliphatic amines, the dispersion of MWCNTs and ultimately mechanical, thermal, and conductive properties of epoxy-based composites could be adjusted. Using an optimal secondary amine number of aliphatic amine (triethylenetetramine), the interlaminar shear strength, tensile strength, and flexural strength of epoxy-based composite increased by 43.9%, 34.8%, and 35.0%, respectively; the work of fracture after interlaminar shear tests increased by 233.9%, suggesting strengthening/ toughening effects of functionalized MWCNTs; significant reduction in surface resistance and increased thermal conductivity were also obtained, implying the superior conductive properties for composites. This work offers a new strategy for designing fiber-reinforced composites with high strength, excellent antistatic properties, and good thermal conductivity for medical device applications.

**Keywords:** carbon nanotubes, glass fiber, surface treatments, interface, mechanical properties, conductive properties

## 1 Introduction

Glass fiber reinforced polymer composite (GFRP) has been widely applied as structural components for many industrial fields, such as medical device, automotive, architectural, and aerospace, because of its advantages of high specific strength, excellent corrosion resistance, and low cost (1–3). However, weak interface properties between glass fiber (GF) and polymer are still restricting GFRP's applications. Moreover, the improvement in mechanical and thermal properties alone can no longer meet the growing needs of material science. Therefore, how to strengthen the fiber/matrix interface and also give such composites multifunctionality (e.g., conductivity) have been urgent problems (4–6). In order to alleviate this problem, a practical strategy is to incorporate some functional nanofillers (e.g., graphene, boron nitride, and silicon carbide) into GFRP (7–10).

Among these functional nanofillers, carbon nanotubes have become one of the ideal fillers because of their excellent properties, such as excellent thermal conductivity, high specific modulus, and magnetic shielding (11,12). In particular, commercial multiwalled carbon nanotubes (MWCNTs) have been accepted for their high-performance cost ratios. Recently, an efficient strategy for introducing carbon nanotubes into GFRP is to deposit carbon nanotubes onto the fiber surfaces via chemical vapor deposition (13,14), electrophoretic deposition (15,16), layer-by-layer assembly (17), and sizing coating (18). This strategy can simultaneously resolve three kinds of problems: enhancing fiber/matrix interface adhesion; reducing the possibility of increased resin viscosity (19), MWCNTs' re-agglomeration (20,21), and filtering by woven fibers (22) during the composite fabrication process; and transferring stress, heat, and electricity efficiently from matrix to fiber or matrix (23). However, carbon nanotubes are easy to be entangled and agglomerated together because of their large specific surface area and high aspect ratios. Improvement in the carbon nanotubes' dispersion is the key to achieve their

<sup>\*</sup> Corresponding author: Yue Li, Department of Gastroenterology, The Second Hospital of Anhui Medical University, Hefei 230601, China, e-mail: misliyue@126.com

**Shaohua Zeng:** Anhui Province Key Laboratory of Environment-Friendly Polymer Materials, School of Chemistry & Chemical Engineering, Anhui University, Hefei 230601, China

excellent enhancing effect for composites. Generally, covalent or non-covalent modification of carbon nanotubes can give them various active groups (e.g., hydroxyl, carboxyl, and amino groups) onto the carbon skeletons (24,25). These surface treatments not only effectively improve the dispersibility of carbon nanotubes, but also enhance the interfacial interactions between carbon nanotubes and polymer matrix.

Epoxy resin is one of the commonly used matrixes for GFRP (26-30). During epoxy-amine curing systems, organic amine-functionalized carbon nanotubes are often used, which contributes to the chemical crosslinking between amine-functionalized carbon nanotubes and epoxy matrix (31,32). Recent research works focus on depositing aminefunctionalized carbon nanotubes onto the GF. For examples, Rahman et al. (33) optimized mechanical and thermomechanical properties of E-glass fabric/epoxy composites by utilizing amino group-containing MWCNTs. It was found that both flexural strength and modulus of 0.3 wt% MWCNTs-filled composites had a maximum enhancement of 38% and 22% in comparison to the control sample. Li et al. (34) deposited 3-aminopropyltrimethoxysilane-functionalized MWCNTs on the woven GF and found that an increase of 23.6% in interlaminar shear strength (ILSS) and an improvement of 35.0-55.4% in thermal conductivity were obtained for MWCNTs-filled composites. Roy et al. (35) reported a doubly modified MWCNTs derivative, in which MWCNTs were first covalently functionalized with oleyl amine and then non-covalently wrapped with polycarbosilane, for reinforcing GF/epoxy composites. It was found that the doubly modified MWCNTs could improve the tensile strength of resultant composites by 23% in comparison to the control sample. However, only few investigations have been involved in the effects of organic amine compositions (chain structure, number of amino groups, etc.) on the interfacial properties of GFRP still.

In this work, a series of aliphatic amines (containing various secondary amine numbers) were selected to functionalize MWCNTs, and then these functionalized MWCNTs were deposited on the surface of GF fabrics. A thorough investigation was conducted into the effects of aliphatic amine-functionalized MWCNTs on the interfacial adhesion and mechanics of the resulting composites. The obtained results indicated amine-functionalized MWCNTs not only improved the mechanical properties of composites, but also gave them good anti-static and heat dissipation properties.

## 2 Materials and methods

## 2.1 Preparation of carbon nanotubesmodified GF reinforcer

All the chemicals, including bismuth chloride, N,N-dimethylformamide (DMF), anhydrous ethanol (chemically pure), ethylenediamine, diethylenetriamine, triethylenetetramine (TETA), tetraethylenepentamine, N,N-diisopropylcarbodiimide (DIC), and 1-hydroxybenzotriazole (HoBt), were purchased from Chemical Reagent Co., Ltd (Nanjing, China). The preparation procedure of MWCNTs-modified GF reinforcer (using ethylenediamine-functionalized MWCNTs as an example) is as follows. First, 1.0 g carboxyl MWCNTs (Chengdu Organic Chemicals Co., Ltd, China; industrial grade, 20–40 nm external diameter, 30 µm length, 1.43 wt% –COOH content) were added into a solution of DMF (0.05 L) containing 0.5 g DIC and 0.5 g HoBt, and mixed homogeneously and then placed in a 600 W ultrasonic bath for 45 min, to obtain MWCNTs suspension. Then, ethylenediamine (1.5 g) was added to the above suspension, followed by stirring for 36 h at room temperature (RT). The reactants were filtered and anhydrous ethanol was used to wash the reactants three times. After drying in a 90°C vacuum for 8 h, ethylenediamine-functionalized MWCNTs were obtained and marked as MWCNTs-a<sub>1</sub>. Using a similar process, diethylenetriamine, TETA, and tetraethylenepentamine were utilized to functionalize carboxyl MWCNTs, respectively; the obtained amine-functionalized MWCNTs were labeled as MWCNTs-a<sub>2</sub>, MWCNTs-a<sub>3</sub>, and MWCNTs-a<sub>4</sub>, respectively.

In anhydrous ethanol, 0.05 g of the prepared aminefunctionalized MWCNTs were diffused with the help of a 600 W ultrasound bath for 45 min, to obtain the MWCNTs suspension with a concentration of  $0.5 \,\mathrm{g}\cdot\mathrm{L}^{-1}$ . The pre-dried E-GF fabric (Saertex Wagener GmbH & Co KG, Germany: areal density: 1,200 g·m<sup>-2</sup>, fiber diameter: ~17 μm) with a size of 200 mm × 300 mm was soaked in the prepared suspension of MWCNTs, followed by an operation with a 600 W ultrasonic bath for 6 min. A MWCNTs-modified GF fabric was obtained after vacuum drying at 90°C for 8 h. Using a similar process, the GF fabric modified by MWCNTs-a<sub>1</sub>, MWCNTs-a<sub>2</sub>, MWCNTs-a<sub>3</sub>, and MWCNTs-a<sub>4</sub> were obtained and marked as M-a<sub>1</sub>-G, M-a<sub>2</sub>-G, M-a<sub>3</sub>-G, and M-a<sub>4</sub>-G, respectively. Figure 1 depicts the scheme to prepare aliphatic amines-functionalized MWCNTs and GF reinforcers.

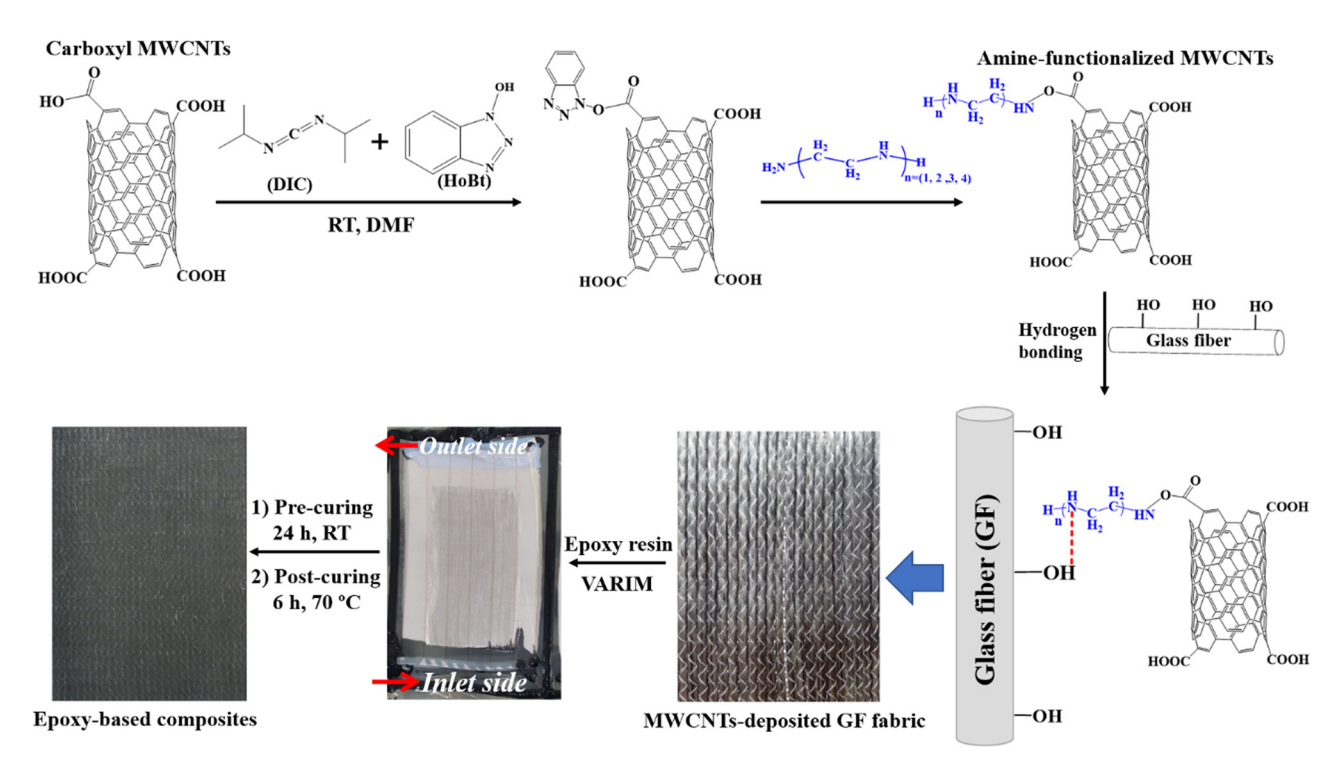


Figure 1: Schematic of synthesis of aliphatic amine-functionalized MWCNTs and preparation of corresponding MWCNTs-modified GF reinforcers.

# 2.2 Fabrication of GF fabric/epoxy composites

The GF fabric/epoxy composite was fabricated by vacuumassisted resin infusion molding (VARIM). First, several layers of MWCNTs-modified GF reinforcers were placed in a homemade sealed VARIM unit, and the airtightness of the device was checked. Then, bisphenol-A epoxy resin (Huntsman Advanced Materials Americas Inc.; LY1564, 1,200-1,400 mPa·s viscosity at 25°C) and amine hardener (Huntsman Advanced Materials Americas Inc.; Aradur 3486, 10-20 mPa·s viscosity at 25°C) (LY1564: Aradur 3486 = 100:34, mass ratio) were evenly mixed, and the mixture was pumped into the VARIM device gradually until resin was fully saturated with MWCNTs-modified GF reinforcers. Finally, the epoxy mixture was pre-cured at RT for 24 h and then at 70°C for 6 h, to obtain MWCNTs-modified GF fabricreinforced epoxy composites. Using a similar process, the epoxy-based composite fabricated by M-a<sub>1</sub>-G, M-a<sub>2</sub>-G, M-a<sub>3</sub>-G, and M-a<sub>1</sub>-G were recorded as M-a<sub>1</sub>-G/E, M-a<sub>2</sub>-G/E, M-a<sub>2</sub>-G/E, and M-a<sub>4</sub>-G/E, respectively. In addition, pure GF fabric-reinforced epoxy composites (G/E) were used as a baseline sample.

#### 2.3 Characterization

Fourier-transform infrared spectroscopy (FTIR; Vertex 80 v FT-IR, Bruker, Germany) was used to check the functionalized MWCNTs with 500-4,000 cm<sup>-1</sup> wavenumbers. X-ray photoelectron spectroscopy (XPS; ESCALAB 250Xi, Thermo Fisher Scientific, USA) was employed for evaluating the functionalized MWCNTs under inert atmosphere. The dispersion degree of MWCNTs on the surface of GFs and fracture surfaces of epoxy-based composites were characterized by field-emission scanning electron microscopy (FESEM; SU8010, Hitachi, Japan). The dispersion degree of MWCNTs in epoxybased composites was also evaluated by high-resolution transmission electron microscopy (TEM; JEM 2100, JEOL, Japan).

All the mechanical properties of epoxy-based composites were performed on a universal testing machine (CMT-5105, Shenzhen Sans, Inc., China) at RT, referring to ISO 527:1997, ISO 14125:1998, and ISO 14130:1997, respectively. The tensile specimens (250 mm × 25 mm × 2 mm) were determined with a crosshead speed of 2.0 mm·min<sup>-1</sup>, referring to ISO 527:1997. The flexural specimens (40 mm imes 15 mm imes2 mm) were determined in the three-point bending mode with a crosshead speed of 2.0 mm·min<sup>-1</sup>, and the span was 32 mm, referring to ISO 14125:1998. The interlaminar shear specimens (40 mm × 20 mm × 4 mm) were determined with a crosshead speed of 1.0 mm·min<sup>-1</sup>, and the span was 20 mm, referring to ISO 14130:1997. An effective experimental datum was obtained based on the test of five specimens.

Viscoelastic behavior of epoxy-based composites was characterized by a dynamic mechanical thermal analyzer (DMTA; Q800, TA Instruments, USA). The DMTA specimens (60 mm × 10 mm × 2 mm) were determined in the three-point bending mode (1 Hz) from RT to 200°C, and the temperature ramp experiment was used at a heat rate of 5°C·min<sup>-1</sup>. Based on the DMTA results, two key factors, including interfacial adhesion factor ( $\alpha$ ) and cross-link density ( $\nu_{\rm e}$ ; mol·L<sup>-1</sup>), could be obtained, respectively. The  $\alpha$  could be used to assess the interface adhesion of epoxybased composites, which was calculated using Eq. 1. A high  $\alpha$  value indicates a strong interfacial adhesion.

$$(\tan \delta_{\max})_c = (\tan \delta_{\max})_m - \alpha V_f \tag{1}$$

where the  $\tan \delta_{\rm max}$  refers to the peak of the loss factor vs temperature curve; the subscript c = composite, subscript m = matrix, subscript f = fiber;  $V_{\rm f}$  = fiber volume fraction, which was obtained by a calcination method.

Moreover, the  $\nu_e$  could be used to evaluate the chemical bonding degree between MWCNTs and matrix. From the rubber elasticity theory, the  $\nu_e$  can be calculated using Eq. 2 (36.37).

$$v_{\rm e} = \frac{E_{\rm r}'}{3RT} \tag{2}$$

where  $E'_{\rm r}$  = storage modulus (*E*') at  $T_{\rm g}$  + 40°C (Pa), T = absolute temperature at  $T_{\rm g}$  + 40°C (K), and R = gas constant (8.314 L·kPa·K $^{-1}$ ·mol $^{-1}$ ). A high  $\nu_{\rm e}$  value reveals more crosslinking points within epoxy matrix.

Surface resistivity of epoxy-based composites was tested by a surface resistance tester (SL-030B, Wuxi Xinlutu Antistatic Equipment Co., Ltd, China), which was used to characterize the anti-static properties of epoxy-based composites. Thermal measurement of epoxy-based composites was carried out using a thermal conductivity analyzer (DZDR-S, Nanjing Dazhan Institute of Electromechanical Technology, China), and infrared thermal imager (Ti450, Fluke, USA). The dimension of these specimens was 4 mm × 40 mm × 40 mm. An effective experimental datum was obtained based on the test of five specimens.

#### 3 Results and discussion

## 3.1 Surface and morphology of MWCNTsmodified GF reinforcer

To evaluate the bonding between aliphatic amines and carboxyl MWCNTs, FTIR and XPS technologies were conducted, and their results are described in Figure 2. As shown in Figure 2(a), the existence of a single peak at 3,436 cm<sup>-1</sup> may be due to the overlap of the two groups stretching vibrational peaks from the hydroxyl group (–OH) of the

carboxyl MWCNTs and the secondary amine (-NH-) of the aliphatic amine. A characteristic absorption of carbonyl groups (C=0) can be observed at 1,705 cm<sup>-1</sup>, which comes from carboxyl groups (-COOH) of carboxyl MWCNTs. Also, the peaks at 1,640 and 1,157 cm<sup>-1</sup> correspond to in-plane shear vibration of -NH- and out-of-plane bending vibration of C-N, respectively. Furthermore, the peaks at 2,931, 2,853, and 1,462 cm<sup>-1</sup> are attributed to the stretching vibration and bending vibration of methylene ( $-CH_2-$ ), which mainly comes from aliphatic amines. With increasing secondary amine amounts in aliphatic amines, the peak intensities of both -NH- and  $-CH_2-$  exhibit an increasing trend. These results indicate that aliphatic amines have been chemically linked to the surface of carboxyl MWCNTs based on amide bonds.

Figure 2(b) shows the analysis of the XPS spectra of functionalized MWCNTs, which further confirms the linkage between the aliphatic amines and the carboxyl MWCNTs through covalent bonding interactions. From Figure 2(b), it can be seen that both carboxyl MWCNTs and MWCNTs-a3 (using TETA-functionalized MWCNTs as an example) show two significant peaks at 533 and 285 eV, which are due to O1s and C1s peaks, respectively. Compared with carboxyl MWCNTs, a new N1s peak at 400.5 eV appears for MWCNTsa<sub>3</sub>, which is caused by the introduction of TETA. By further analysis of the N1s peak, two binding energy (BE) peaks are observed (Figure 2(c)), corresponding to amide nitrogen peak (400.7 eV) and amine nitrogen peak (400.0 eV). Comparatively speaking, the higher BE value for amide nitrogen is attributed to the formation of a conjugate bond between nitrogen and carbonyl groups in amide groups. In addition, the peak intensities of amide nitrogen and amine nitrogen are essentially the same, indicating that only one amino group is bonded to carboxvl MWCNTs.

The dispersion of aliphatic amine-functionalized MWCNTs on the surface of GFs is exhibited in Figure 3. The clean surface of pure GF is protected by the original sizing coats (Figure 3(a)). The distribution of all aliphatic amine-functionalized MWCNTs on the fiber surface is relatively homogeneous, but some MWCNT aggregates are still visible on the M-a<sub>1</sub>-GF surface (Figure 3(b)), indicating poor modified effect for ethylenediamine. With the increase in secondary amine amounts in aliphatic amines, more homogeneous dispersion of functionalized MWCNTs is observed, especially for TETA-functionalized MWCNTs in M-a<sub>3</sub>-G (Figure 3(d and d')). These results indicate that aliphatic amines containing appropriate secondary amine amounts are beneficial to improve the dispersibility of MWCNTs. On the one hand, the increased secondary amine amounts on the MWCNTs, surface can enhance the electrostatic repulsion among functionalized MWCNTs and thereby reduce the reunion of MWCNTs. On the other hand,

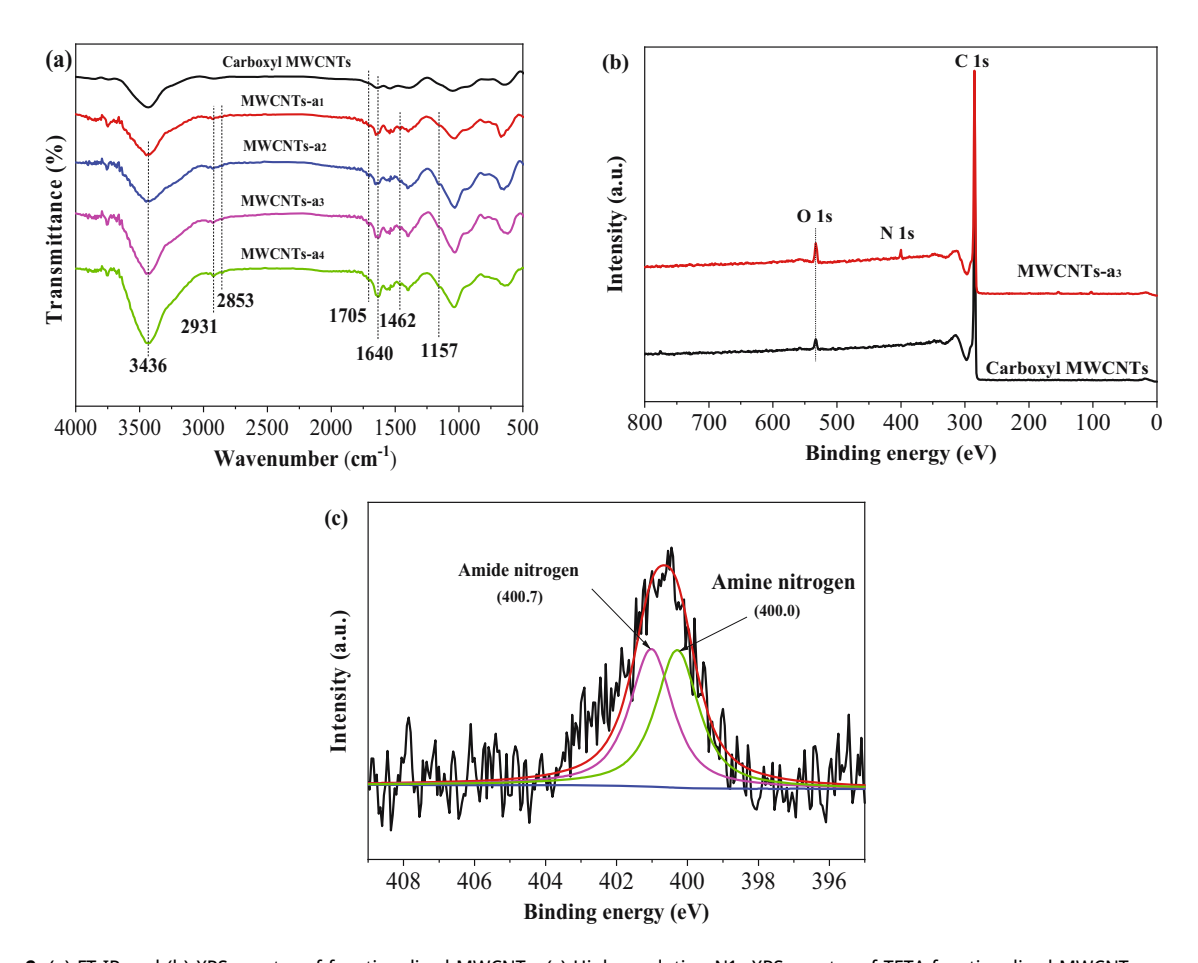


Figure 2: (a) FT-IR and (b) XPS spectra of functionalized MWCNTs. (c) High-resolution N1s XPS spectra of TETA-functionalized MWCNTs.

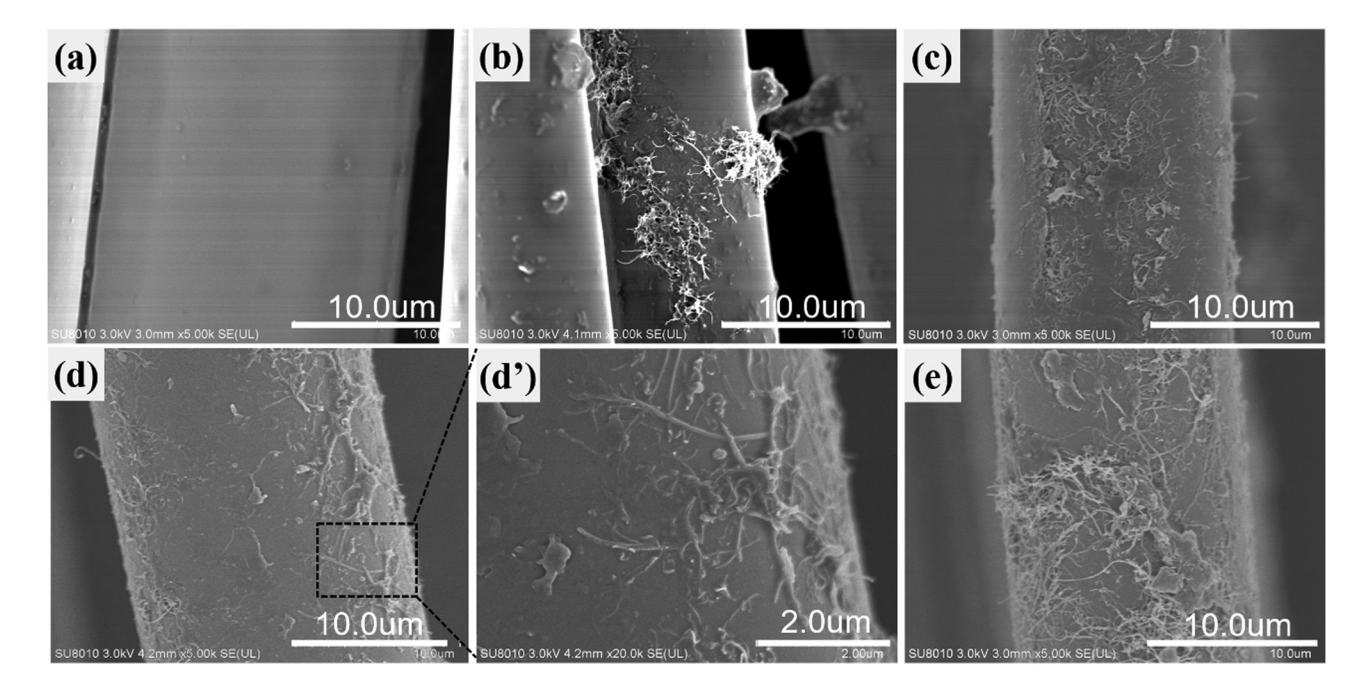


Figure 3: SEM images of dispersion of aliphatic amine-functionalized MWCNTs onto GF surface: (a) GF, (b) M-a<sub>1</sub>-G, (c) M-a<sub>2</sub>-G, (d and d') M-a<sub>3</sub>-G for different magnification and (e) M-a<sub>4</sub>-G.

they provide more opportunities for hydrogen bonding between MWCNTs and GFs, and thus allow MWCNTs to be more easily adsorbed by the fiber surface.

# 3.2 Interlaminar properties of epoxy-based composites

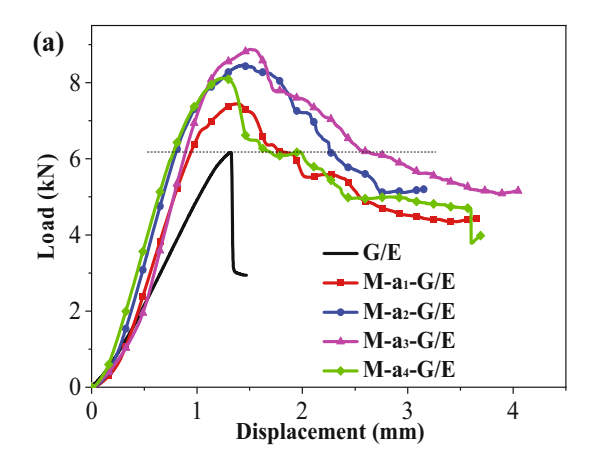
Interlaminar shear behavior is an important property for revealing the interfacial adhesion of composites. Figure 4 displays the load–displacement curves, ILSS, and work of fracture ( $W_f$ ) of epoxy-based composites containing aliphatic amine-functionalized MWCNTs. The  $W_f$  is a common factor to evaluate interlaminar fracture toughness of epoxy-based composites. To obtain the  $W_f$ , pure G/E's peak load is selected as the horizontal line and intersects with the load drop curve of epoxy-based composites with functionalized MWCNTs. The surrounded area under the load–displacement curve was calculated as the  $W_f$  value.

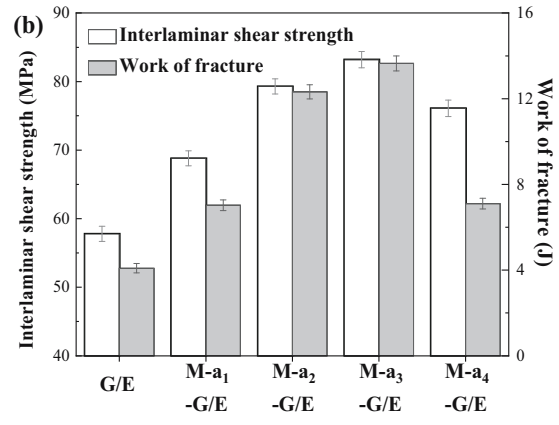
For pure G/E, the load–displacement curve rises slowly to peak and then drops suddenly (Figure 4(a)). It indicates that pure G/E exhibits a brittle disruption under the interlaminar shear force. In contrast, all the load–displacement curves of epoxy-based composites containing aliphatic amine-functionalized MWCNTs show a tendency to decline slowly after the peaks. It can be explained that aliphatic amine-functionalized MWCNTs can enhance the interlaminar adhesion between adjacent composite interlayers and thus inhibit the delamination failure of composites. Furthermore, both ILSS and  $W_{\rm f}$  of epoxy-based composites tend to increase and then decrease with increase in the secondary amine amounts, and a peak value is seen for M-a<sub>3</sub>-G/E. In comparison to pure G/E, ILSS and  $W_{\rm f}$  of M-a<sub>3</sub>-G/E. In comparison to pure G/E, ILSS and  $W_{\rm f}$  of M-a<sub>3</sub>-

G/E are improved by 43.9% and 233.9%, respectively. This phenomenon shows that too small number of secondary amines in aliphatic amines is not enough to improve the resin cross-linking density, but excessive secondary amines lead to the brittleness of epoxy matrix. Only appropriate number of secondary amines in aliphatic amines can enhance the interlaminar adhesion strength of G/E. Moreover, TETA-functionalized MWCNTs with uniform dispersion in the interlaminar region can efficiently transfer and dissipate stress between adjacent composite interlayers and thereby enhance interlaminar fracture toughness of composites.

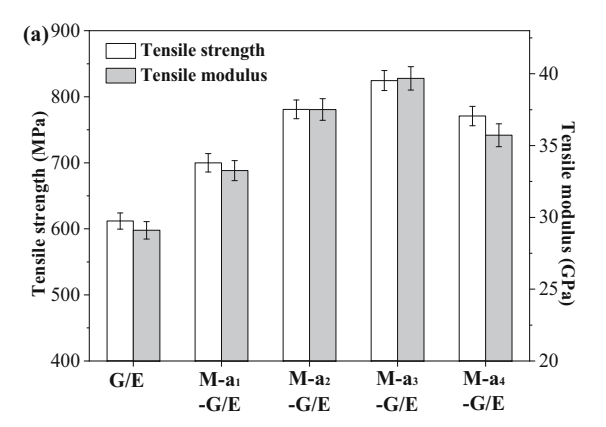
# 3.3 Tensile and flexural properties of epoxybased composites

The amount of active secondary amines on the functionalized MWCNTs surface can directly determine the cross-linking density of resin and thus affect mechanical properties of resultant composites. Figure 5 shows the tensile and flexural characteristics of epoxy-based composites containing aliphatic amine-functionalized MWCNTs. In comparison to pure G/E, both strength and modulus of functionalized MWCNTs-filled epoxy-based composites increase, following the overall order of M-a<sub>3</sub>-G/E > M-a<sub>2</sub>-G/E > M-a<sub>4</sub>-G/E > M-a<sub>1</sub>-G/E. Additionally, the tensile strength ( $\sigma_t$ ) and modulus ( $E_t$ ) of M-a<sub>4</sub>-G/E have the maximum values, which are raised by 34.8% and 36.4%, respectively, and relevant flexural strength  $(\sigma_f)$  and modulus  $(E_f)$  are raised by 35.0% and 46.8%, respectively, in comparison to pure G/E. Appropriate number of secondary amines can not only effectively promote the dispersion degree of MWCNTs in composites, but also directly participate in the cross-linking reaction between MWCNTs





**Figure 4:** Interlaminar shear properties of epoxy composites containing aliphatic amine-functionalized MWCNTs: (a) load–displacement curves and (b) interlaminar shear strength and work of fracture.



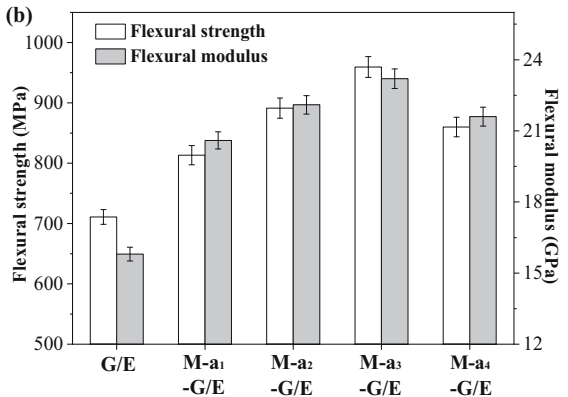


Figure 5: (a) Tensile properties and (b) flexural properties of epoxy composites containing aliphatic amine-functionalized MWCNTs.

and matrix, both of which strengthen epoxy-based composites. However, excess secondary amines on MWCNTs surface easily arouse a brittle failure for epoxy-based composites.

# 3.4 Dynamic mechanical thermal analysis of epoxy-based composites

For assessing the interfacial micro-mechanical behavior, the dynamic viscoelasticity of epoxy-based composites was performed. Figure 6 illustrates the storage modulus (E), loss modulus (E), and loss factor ( $\tan \delta$ ) vs temperature curves of epoxy-based composites containing functionalized MWCNTs.

As shown in Figure 6(a), the E' values in the glassy and rubber regions of functionalized MWCNTs-filled epoxybased composites are larger than pure G/E, especially in the glassy region. With the increase in number of secondary amines, both E' values at 30°C ( $E'_{30}$ ) and the temperature in the rubbery region ( $E'_{r}$ ) of epoxy-based composites tend to increase first and then decrease. In comparison to pure G/E,  $E'_{30}$  and  $E'_{r}$  of M-a<sub>3</sub>-G/E have the maximum values, which are improved by 32.6% and 127.0%, respectively. It suggests that adding an appropriate quantity of secondary amines can increase the elasticity of composites by increasing the adhesion between the fiber and matrix.

From Figure 6(b), the E'' peak values ( $E''_{max1}$  and  $E''_{max2}$ , respectively) of M-a<sub>2</sub>-G/E, M-a<sub>3</sub>-G/E, and M-a<sub>4</sub>-G/E are lower than pure G/E, except for M-a<sub>1</sub>-G/E. The  $E''_{max1}$  and  $E''_{max2}$  values of M-a<sub>3</sub>-G/E are the lowest in all cases. This result indicates that appropriate aliphatic amine-functionalized MWCNTs can enhance the stress transfer efficiency from matrix to fiber, which further reduces the mechanical loss and slows down the failure of epoxy-based composites.

The thermal stability of epoxy-based composites is also significantly impacted by aliphatic amine-functionalized MWCNTs. The corresponding glass-transition temperatures  $(T_{\rm g})$  and the temperature at the rubbery region  $(T_{\rm r})$  are listed in Table 1. All of the first  $T_{\rm g}$   $(T_{\rm gl})$ , second  $T_{\rm g}$   $(T_{\rm g2})$ , and  $T_{\rm r}$  of epoxy-based composites containing functionalized MWCNTs are greater than those of pure G/E. The M-a<sub>3</sub>-G/E has the maximum  $T_{\rm gl}$ ,  $T_{\rm g2}$  and  $T_{\rm r}$  values, 9.5°C, 4.8°C, and 7.7°C higher than pure G/E. Appropriate number of secondary amines on the MWCNTs surface can improve the interfacial interactions (chemical crosslinking) between functionalized MWCNTs (amino groups) and epoxy matrix (epoxide groups) (31–34). This result effectively restricts the movement of molecular chains on the surface of GFs and thus enhance the thermal stability of epoxy-based composites.

# 3.5 Interfacial adhesion analysis of epoxybased composites

The interfacial adhesion of epoxy-based composites can be reflected by two parameters, the interfacial adhesion factor ( $\alpha$ ) and cross-link density ( $\nu_{\rm e}$ ). The first peak value observed in the loss factor vs temperature curve ( $\tan \delta_{\rm max1}$ ) is used to calculate the  $\alpha$  value, which is listed in Table 2. Compared with pure G/E, the  $\tan \delta_{\rm max1}$  of the composites are significantly reduced and the  $\alpha$  values are significantly raised after adding aliphatic amine-functionalized MWCNTs. Besides, M-a<sub>3</sub>-G/E's  $\alpha$  value is the largest in all the cases, which is an increase of 18.4% than pure G/E. It indicates that the functionalized MWCNTs with appropriate number of secondary amines can enhance the interfacial adhesion of epoxy-based composites. In addition, the  $\nu_{\rm e}$  value of epoxy-based composites increase significantly, and the largest  $\nu_{\rm e}$  value is obtained for the M-a<sub>3</sub>-G/E. In the epoxy-amine resin system,

8 — Yue Li and Shaohua Zeng DE GRUYTER

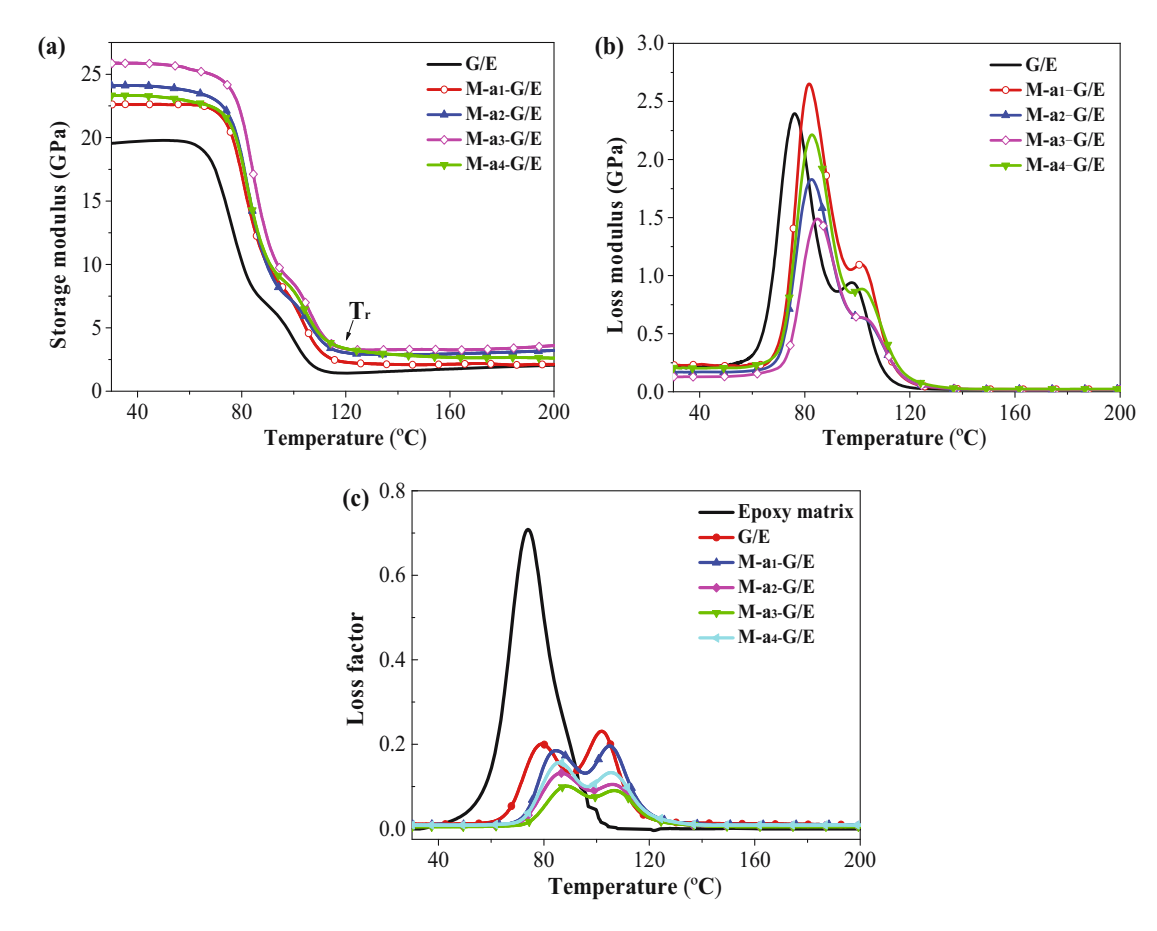


Figure 6: (a) Storage modulus, (b) loss modulus, (c) and loss factor vs temperature curves of epoxy composites containing aliphatic amine-functionalized MWCNTs.

only appropriate amount of secondary amines can effectively participate in the crosslinking reaction with epoxy matrix, so as to improve the  $\nu_e$  of the composite. Excess secondary amines cannot provide more crosslinking points for epoxy matrix.

Figure 7 shows shear fracture surfaces of functionalized MWCNTs-filled epoxy-based composites after interlaminar shear testing. As seen in Figure 7(a), the shear fracture surface of pure G/E is smooth, and the matrix is completely de-bonded from GFs, indicating poor interface

**Table 2:**  $\tan \delta_{\max}$  and  $\alpha$  values of epoxy composites containing aliphatic amine-functionalized MWCNTs

Samples	V <sub>f</sub> (%)	tan $\delta_{ ext{max1}}$	α (×10 <sup>-3</sup> )	ν <sub>e</sub> (mol·L <sup>-1</sup> )	
Epoxy matrix	-	0.708	_	_	
Pure G/E	52.1 ± 0.5	0.201	9.8	1.549	
M-a₁-G/E	52.2 ± 0.7	0.185	10.0	2.169	
M-a <sub>2</sub> -G/E	52.4 ± 0.6	0.132	11.0	2.223	
M-a <sub>3</sub> -G/E	52.3 ± 0.5	0.101	11.6	2.432	
M-a <sub>4</sub> -G/E	52.1 ± 0.6	0.157	10.6	2.267	

 $\textbf{Table 1:} \ \textit{E'}, \ \textit{T}_g, \ \text{and} \ \textit{T}_r \ \text{of epoxy composites containing aliphatic amine-functionalized MWCNTs}$ 

Sample	Storage modulus (GPa)		Loss modulus (GPa)		T <sub>g1</sub> (°C)	T <sub>g2</sub> (°C)	T <sub>r</sub> (°C)
	E' <sub>30</sub>	$E_{ m r}'$	E" <sub>max1</sub>	E" <sub>max2</sub>			
Pure G/E	19.5	1.44	2.40	0.94	79.2	101.9	116.8
M-a <sub>1</sub> -G/E	22.6	2.44	2.65	1.10	84.7	104.9	122.9
M-a <sub>2</sub> -G/E	24.1	2.95	1.83	0.66	86.6	105.9	123.8
M-a <sub>3</sub> -G/E	25.9	3.26	1.49	0.64	88.7	106.7	124.5
M-a <sub>4</sub> -G/E	23.3	3.21	2.21	0.89	85.9	105.6	124.1

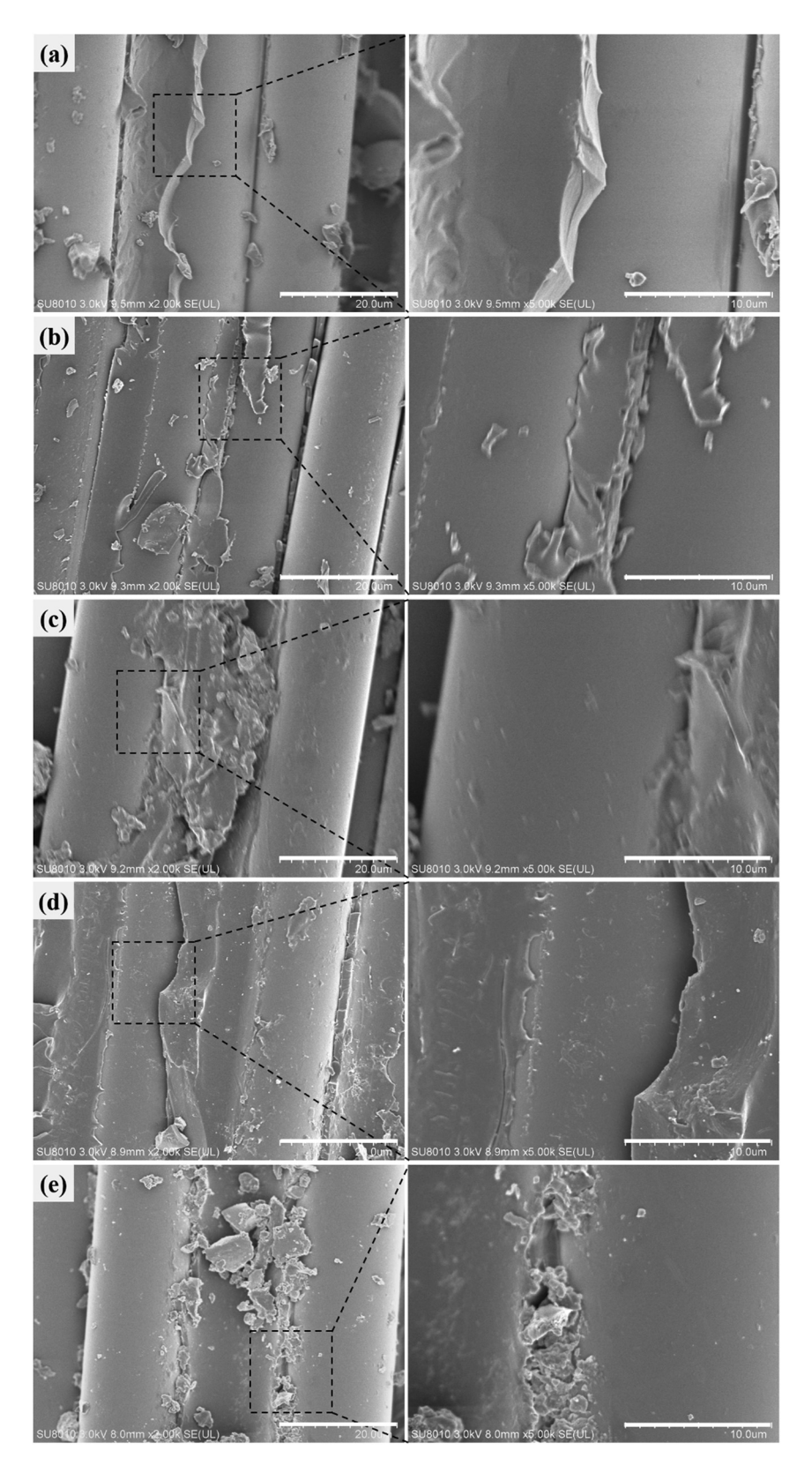
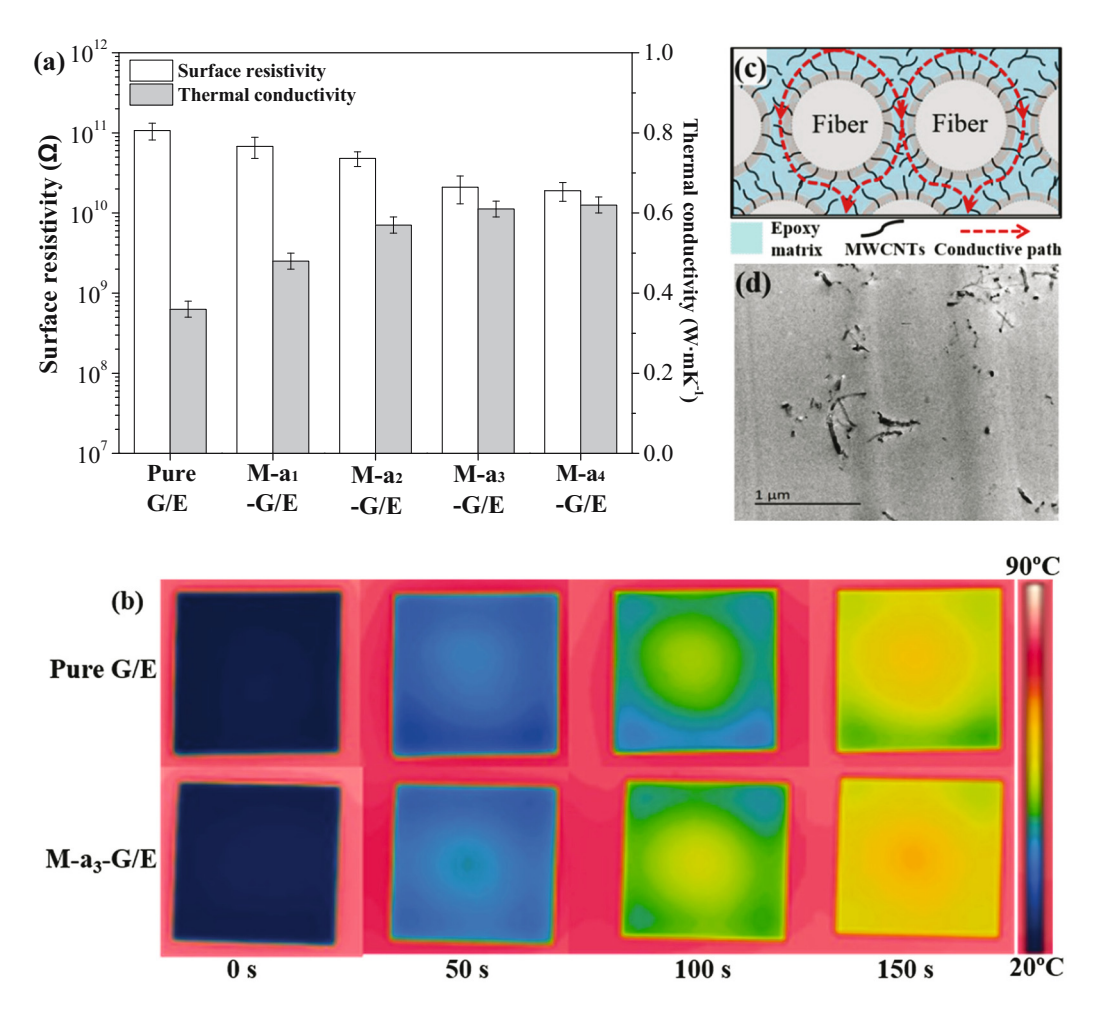


Figure 7: Shear fracture surfaces of epoxy composites containing aliphatic amine-functionalized MWCNTs: (a) G/E, (b) M-a<sub>2</sub>-G/E, (c) M-a<sub>3</sub>-G/E, (d) M- $a_4$ -G/E, and (e) M- $a_5$ -G/E.



**Figure 8:** (a) Surface resistivity and thermal conductivity, (b) infrared thermal images of composites, (c) schematic of conductive paths in composite cross section, and (d) TEM image of TETA-modified MWCNTs at the fiber/matrix interface.

adhesion. In comparison to pure G/E, the cross-sectional morphology of functionalized MWCNTs-filled epoxy-based composites show more resin fragments (Figure 7(b)–(e)). In particular, epoxy matrix of M-a<sub>3</sub>-G/E exhibit a ductile failure. These results indicate that appropriate aliphatic amine-functionalized MWCNTs on fiber surface can provide an effective mechanical interlocking with epoxy matrix, which improves fiber/matrix interfacial adhesion; meanwhile, uniformly dispersed MWCNTs can effectively transfer/dissipate stress, which helps in toughening epoxy-based composites.

# 3.6 Conductive analysis of epoxy-based composites

Epoxy-based composites occasionally require to have good electrical conductivity to disperse heat or to dissipate static as medical equipment are utilized with increasing precision, which guarantees safe and efficient operation of medical devices. Based on the high conductivity characteristics of carbon nanotubes, the electrical or heat conductivity of epoxy-based composites are expected to be improved (38). The surface resistivity and thermal conductivity of functionalized MWCNTs-filled epoxy-based composites are displayed in Figure 8.

It is clear that functionalized MWCNTs play a part in improving the conductivity of the resultant epoxy-based composites. From Figure 8(a), with the increase in the number of secondary amines, the surface resistivity of epoxy-based composites exhibits a down-trend, suggesting the increased anti-static function; moreover, the thermal conductivity of corresponding composites shows an uptrend, revealing the enhanced heat dissipation effect. The minimum surface resistivity and the maximum thermal conductivity is obtained for M-a<sub>4</sub>-G/E; the conductivity of M-a<sub>3</sub>-G/E is next to that of M-a<sub>4</sub>-G/E. As observed in Figure 8(b), the well heat dissipation effect of epoxy-based composites is

visually displayed from infrared thermal images, in which the surface temperature of M-a<sub>3</sub>-G/E rapidly rises to the maximum at the same time (e.g., 150 s). The dispersion degree of functionalized MWCNTs in composites has been greatly improved, as observed in Figure 8(d). These results indicate that appropriate secondary amine numbers play a positive role in promoting the MWCNTs' dispersion and thus raise the touching or connecting probability of MWCNTs (39,40), which provides conductive pathways. The formation of these touching or connecting MWCNTs can minimize defects of phonon transport and reduce the resistance along the heat or electronic flow path.

## 4 Conclusion

In this study, carboxyl MWCNTs were functionalized by a series of aliphatic amines containing various secondary amines and then dispersed on the GF surface, followed by a VARIM procedure. The obtained GF/epoxy composites exhibited superior mechanical, thermal, and conductive properties compared to pure GF/epoxy composite. Aliphatic amines were grafted on the surface of MWCNTs via a covalent bonding. Moreover, aliphatic amines containing appropriate secondary amine numbers gave MWCNTs well dispersion state on the GF surface. Well-dispersed MWCNTs anchored on the GF surface provided a mechanical interlocking with epoxy matrix and facilitated the stress/heat/electronic transfer from matrix to fiber. The optimized aliphatic amine for functionalizing MWCNTs was TETA, where the mechanical, thermal, and conductive properties of resultant epoxy-based composites had the peak values. Compared with pure GF/epoxy composite, the ILSS, tensile strength, and flexural strength of resultant epoxybased composite increased by 43.9%, 34.8%, and 35.0%, respectively; the work of fracture after interlaminar shear tests increased by 233.9%; significantly reduced surface resistance and increased thermal conductivity were also obtained.

Funding information: This work was financed by Natural Science Foundation of Anhui Medical University (No. 2021XKJ044) and Anhui Provincial Natural Science Foundation (No. 2108085QE201).

Author contributions: Yue Li: conceptualization, formal analysis, methodology, funding acquisition, writing - original draft; Shaohua Zeng: conceptualization, data curation, visualization, investigation, funding acquisition, and writing - review and editing.

**Conflict of interest:** Authors state no conflict of interest.

## References

- Somaiah Chowdary M, Raghavendra G, Kumar MSRN, Ojha S, (1) Mohan Kiran P, Panchal M. A comparison of the effect of nano clay addition on microstructures and mechanical properties of epoxy and polyester reinforced glass/sisal hybrid polymer composites. Polym Compos. 2022;43(6):3871-9. doi: 10.1002/pc.26662.
- Pearson A, Duncan M, Hammami A, Naguib HE. Interfacial adhe-(2) sion and thermal stability of high-density polyethylene glass fiber composites. Compos Sci Technol. 2022;227:109570. doi: 10.1016/j. compscitech.2022.109570.
- Xie J. Effect of matrix composition on properties of polyamide 66/ polyamide 6I-6T composites with high content of continuous glass fiber for optimizing surface performance. e-Polymers. 2023;23(1):20228111. doi: 10.1515/epoly-2022-8111.
- Gao X, Yang W, Tan J, Song L, Cheng L, Tian X. Structural, electrical, and electromagnetic shielding properties of nanocarbon-coated glass fiber-reinforced polypropylene. Polym Compos. 2022:43(5):2796-802. doi: 10.1002/pc.26576.
- Kim D-K, Choi YH, Kim K-W, Kim B-J. Transparent glass-fiber-reinforced epoxy composites and their optical characteristics. Compos Sci Technol. 2023;232:109848. doi: 10.1016/j.compscitech.2022. 109848.
- (6) Rahmani H, Najaf SHM, Ashori A, Golriz M. Elastic properties of carbon fibre-reinforced epoxy composites. Polym Polym Compos. 2015;23(7):475-82. doi: 10.1177/096739111502300706.
- Satish Kumar D, Sathish T, Mavinkere Rangappa S, Boonyasopon P, Siengchin S. Mechanical property analysis of nanocarbon particles/ glass fiber reinforced hybrid epoxy composites using RSM. Compos Commun. 2022;32:101147. doi: 10.1016/j.coco.2022.101147.
- Dasari S, Patnaik S, Ray BC, Prusty RK. Effects of in-situ cryogenic testing temperature and ex-situ cryogenic aging on the mechanical performance of glass fiber reinforced. polymer composites with waste short carbon fibers as secondary reinforcements. Polym Compos. 2023;44(1):294-304. doi: 10.1002/pc.27045.
- Hua Y, Li F, Hu N, Fu S-Y. Frictional characteristics of graphene oxide-modified continuous glass fiber reinforced epoxy composite. Compos Sci Technol. 2022;223:109446. doi: 10.1016/j.compscitech. 2022.109446.
- Ashori A, Ghiyasi M, Fallah A. Glass fiber-reinforced epoxy composite with surface-modified graphene oxide: Enhancement of interlaminar fracture toughness and thermo-mechanical performance. Polym Bull. 2019;76(1):259-70. doi: 10.1007/s00289-018-
- (11) Wu Y, Chen L, Han Y, Liu P, Xu H, Yu G, et al. Hierarchical construction of cnt networks in aramid papers for high-efficiency microwave absorption. Nano Res. 2023;16(5):7801-9. doi: 10.1007/ s12274-023-5522-4.
- (12)Guo L, Xu H, Wu N, Yuan S, Zhou L, Wang D, et al. Molecular dynamics simulation of the effect of the thermal and mechanical properties of addition liquid silicone rubber modified by carbon nanotubes with different radii. e-Polymers. 2023;23(1):20228105. doi: 10.1515/epoly-2022-8105.
- (13)He DL, Salem D, Cinquin J, Piau G-P, Bai JB. Impact of the spatial distribution of high content of carbon nanotubes on the electrical conductivity of glass fiber fabrics/epoxy composites fabricated by RTM technique. Compos Sci Technol. 2017;147:107-15. doi: 10.1016/ j.compscitech.2017.05.012.
- Boddu VM, Brenner MW, Patel JS, Kumar A, Mantena PR, Tadepalli T, et al. Energy dissipation and high-strain rate dynamic

- response of e-glass fiber composites with anchored carbon nanotubes. Compos Part B Eng. 2016;88:44-54. doi: 10.1016/j. compositesb.2015.10.028.
- (15) An Q, Tamrakar S, Gillespie JW, Rider AN, Thostenson ET. Tailored glass fiber interphases via electrophoretic deposition of carbon nanotubes: Fiber and interphase characterization. Compos Sci Technol. 2018;166:131-9. doi: 10.1016/j.compscitech.2018.01.003.
- (16) Tamrakar S, An Q, Thostenson ET, Rider AN, Haque BZ, Gillespie IW. Tailoring interfacial properties by controlling carbon nanotube coating thickness on glass fibers using electrophoretic deposition. ACS Appl Mater Interfaces. 2015;8(2):1501-10. doi: 10.1021/acsami. 5b10903.
- (17) Fang J, Zhang L, Li C. Polyamide 6 composite with highly improved mechanical properties by PEI-CNT grafted glass fibers through interface wetting, infiltration and crystallization. Polymer. 2019;172:253-64. doi: 10.1016/j.polymer.2019.03.013.
- (18) da Silva LV, Pezzin SH, Rezende MC, Amico SC. Glass fiber/carbon nanotubes/epoxy three-component composites as radar absorbing materials. Polym Compos. 2016;37(8):2277-84. doi: 10.1002/pc. 23405
- (19) Fan ZH, Advani SG. Characterization of orientation state of carbon nanotubes in shear flow. Polymer. 2005;46(14):5232-40. doi: 10. 1016/j.polymer.2005.04.008.
- (20) Chandrasekaran VCS, Advani SG, Santare MH. Role of processing on interlaminar shear strength enhancement of epoxy/glass fiber/ multi-walled carbon nanotube hybrid composites. Carbon. 2010;48(13):3692-9. doi: 10.1016/j.carbon.2010.06.010.
- (21) Zeng SH, Shen MX, Duan PP, Lu FL, Chen SN, Xue YJ. Effect of ultrasonic-assisted impregnation parameters on the preparation and interfacial properties of MWCNT/glass-fiber reinforced composites. e-Polymers. 2018;18(1):35-47. doi: 10.1515/epoly-2017-0112.
- (22) Seyhan AT, Tanoglu M, Schulte K. Mode I and mode II fracture toughness of e-glass non-crimp fabric/carbon nanotube (CNT) modified polymer based composites. Eng Fract Mech. 2008;75(18):5151-62. doi: 10.1016/j.engfracmech.2008.08.003.
- (23) Zeng SH, Shen MX, Duan PP, Lu FL, Chen SN, Li ZY. Properties of MWCNT-glass fiber fabric multiscale composites: Mechanical properties, interlaminar adhesion, and thermal conductivity. Text Res J. 2018;88(23):2712-26. doi: 10.1177/0040517517729387.
- (24) Ku-Herrera JJ, Avilés F, Nistal A, Cauich-Rodríguez JV, Rubio F, Rubio J, et al. Interactions between the glass fiber coating and oxidized carbon nanotubes. Appl Surf Sci. 2015;330:383-92. doi: 10. 1016/j.apsusc.2015.01.025.
- (25) Zeng SH, Duan PP, Shen MX, Xue YJ, Lu FL, Yang L. Interface enhancement of glass fiber fabric/epoxy composites by modifying fibers with functionalized MWCNTs. Compos Interfaces. 2019;26(4):291-308. doi: 10.1080/09276440.2018.1499354.
- (26) Wang L, Ma Z, Qiu H, Zhang Y, Yu Z, Gu J. Significantly enhanced eectromagnetic interference shielding performances of epoxy nanocomposites with long-range aligned lamellar structures. Nano-Micro Lett. 2022;14(1):224. doi: 10.1007/s40820-022-00949-8.
- (27) Zhong X, Yang X, Ruan K, Zhang J, Zhang H, Gu J. Discotic liquid crystal epoxy resins integrating intrinsic high thermal conductivity and intrinsic flame retardancy. Macromol Rapid Commun. 2022;43(1):2100580. doi: 10.1002/marc.202100580.

- (28) Wang C, Huo S, Ye G, Song P, Wang H, Liu Z. A p/si-containing polyethylenimine curing agent towards transparent, durable firesafe, mechanically-robust and tough epoxy resins. Chem Eng J. 2023;451:138768. doi: 10.1016/j.cej.2022.138768.
- (29) Azhary T, Wildan MW. Mechanical, morphological, and thermal characteristics of epoxy/glass fiber/cellulose nanofiber hybrid composites. Polym Test. 2022;110:107560. doi: 10.1016/j. polymertesting.2022.107560.
- (30) Menbari S, Ashori A, Rahmani H, Bahrami R. Viscoelastic response and interlaminar delamination resistance of epoxy/glass fiber/ functionalized graphene oxide multi-scale composites. Polym Test. 2016;54:186-95. doi: 10.1016/j.polymertesting.2016.07.016.
- (31)Wang Q, Chen S, Zeng S, Chen P, Xu Y, Nie W, et al. Tunable mechanical properties of glass fiber/epoxy composites by incorporating bioinspired montmorillonite-carbon nanotube/epoxy interface layer around the fiber. Compos Part B Eng. 2022;242:110092. doi: 10.1016/j.compositesb.2022.110092.
- (32) Rodriguez AJ, Guzman ME, Lim C-S, Minaie B. Mechanical properties of carbon nanofiber/fiber-reinforced hierarchical polymer composites manufactured with multiscale-reinforcement fabrics. Carbon. 2011;49(3):937-48. doi: 10.1016/j.carbon.2010.10.057.
- (33) Rahman MM, Zainuddin S, Hosur MV, Malone JE, Salam MBA, Kumar A, et al. Improvements in mechanical and thermomechanical properties of e-glass/epoxy composites using amino functionalized MWCNTs. Compos Struct. 2012;94(8):2397-406. doi: 10.1016/j.compstruct.2012.03.014.
- (34) Li J, Wu Z, Huang C, Li L. Multiscale carbon nanotube-woven glass fiber reinforced cyanate ester/epoxy composites for enhanced mechanical and thermal properties. Compos Sci Technol. 2014;104:81-8. doi: 10.1016/j.compscitech.2014.09.007.
- (35) Roy D, Tiwari N, Mukhopadhyay K, Saxena AK. The effect of a doubly modified carbon nanotube derivative on the microstructure of epoxy resin. Polymer. 2014;55(2):583-93. doi: 10.1016/j.polymer. 2013.12.012.
- (36) Darroman E, Bonnot L, Auvergne R, Boutevin B, Caillol S. New aromatic amine based on cardanol giving new biobased epoxy networks with cardanol. Eur J Lipid Sci Technol. 2015;117(2):178–89. doi: 10.1002/ejlt.201400248.
- (37) Ding R, Xia Y, Mauldin TC, Kessler MR. Biorenewable romp-based thermosetting copolymers from functionalized castor oil derivative with various cross-linking agents. Polymer. 2014;55(22):5718-26. doi: 10.1016/j.polymer.2014.09.023.
- (38) Ma R-Y, Yi S-Q, Li J, Zhang J-L, Sun W-J, Jia L-C, et al. Highly efficient electromagnetic interference shielding and superior mechanical performance of carbon nanotube/polydimethylsiloxane composite with interface-reinforced segregated structure. Compos Sci Technol. 2023;232:109874. doi: 10.1016/j.compscitech.2022.109874.
- (39) Wang L, Qiu H, Liang C, Song P, Han Y, Han Y, et al. Electromagnetic interference shielding MWCNT-Fe<sub>3</sub>O<sub>4</sub>@Ag/epoxy nanocomposites with satisfactory thermal conductivity and high thermal stability. Carbon. 2019;141:506-14. doi: 10.1016/j.carbon.2018.10.003.
- (40) Yuan S, Zheng Y, Chua CK, Yan Q, Zhou K. Electrical and thermal conductivities of MWCNT/polymer composites fabricated by selective laser sintering. Compos Part A Appl Sci Manuf. 2018;105:203-13. doi: 10.1016/j.compositesa.2017.11.007.